Mathematical Biosciences and Engineering

http://www.aimspress.com/journal/MBE

Mathematical Biosciences and Engineering, (): xxx–xxx
DOI:
Received: 26 April 2022
Accepted:
Published:

Type of article

Incorporating Vaccination into Compartment Models for Infectious Diseases

Glenn Ledder[1]

[1] Department of Mathematics, University of Nebraska-Lincoln, Lincoln, NE 68588-0130, USA

* **Correspondence:** gledder@unl.edu

Abstract: The standard way of incorporating vaccination into a compartment model for an infectious disease is as a spontaneous transition process that applies to the entire susceptible class. The large degree of COVID-19 vaccine refusal and initial limitations of supply and distribution require reconsideration of this standard treatment. In this paper, we address these issues for models on endemic and epidemic time scales. On an endemic time scale, we partition the susceptible class into prevaccinated and unprotected subclasses and show that vaccine refusal has a significant impact on endemic behavior, particularly for diseases where immunity is short-lived. On an epidemic time scale, we develop a supply-limited Holling type 3 vaccination model and show that it is an excellent fit to vaccination data. We also extend the Holling model to a COVID-19 scenario in which the population is divided into two risk classes, with the high-risk class being prioritized for vaccination. For both cases with and without stratification by risk, we see significant differences in epidemiological outcomes between the Holling vaccination model and naive models. Finally, we use the new model to explore implications for public health policies in future pandemics.

Keywords: vaccination, COVID-19, compartment models, epidemic disease models, endemic disease models

1. Introduction

Vaccination is generally incorporated into dynamical system disease models as a single-phase spontaneous transition process that ultimately moves everyone out of the susceptible class who does not contract the disease first [2, 4, 18]. These assumptions are questionable on two grounds: first, the significant level of resistance to vaccination against COVID-19 suggests that vaccine refusal needs to be incorporated into infectious disease models; second, the dynamics of the single-phase spontaneous transition does not match the dynamics of vaccination during the rollout of a new vaccine.

In a single-phase spontaneous transition, the rate is proportional to the size of the leaving class. This assumption is mathematically convenient, but it is often biologically inaccurate. In a true spontaneous

transition, such as radioactive decay, the absolute rate of transition in a collection of individuals is largest at the beginning, when the collection itself is largest. This is not true for disease processes such as recovery, where a mean time of 5 days means that most transitions occur in days 4, 5, and 6. The modeling error caused by using a spontaneous transition for recovery in an endemic disease model is small because the overall rate at steady state is dependent primarily on the mean time and not the distribution of times. For an epidemic model, we often assume spontaneous transitions in spite of the modeling error; alternatively, we could use a multi-phase transition model, corresponding to an Erlang distribution of times [1, 14]. In this way, we can control the standard deviation of the transition time as well as the mean.

For vaccination in a model for a novel disease, the problem with assuming spontaneous transition is different in character. Those of us who wanted to be vaccinated as soon as a vaccine was approved found that we could not get our shots until our risk class was cleared; even then, the waiting time for an appointment was sometimes long. A spontaneous transition model imposes no limit to the number of transitions that can occur simultaneously, whereas in vaccination there is a hard limit to the number of appointment slots, one which is initially low because of supply limitations and saturates to the capacity of the administrative system. A better model will need to account for both limited supply and limited distribution capacity.

The issues raised here play out differently depending on the time scale of the model. Problems of supply and distribution are important on an epidemic time scale of weeks to months, but not on an endemic time scale of years. For endemic models, the primary concern with the standard treatment of vaccination is vaccine refusal, which probably will not abate significantly over time. We consider this issue in Section 2 by considering the impact of vaccine refusal in a variant of the standard SIR endemic model that incorporates vaccination, vaccine refusal, and loss of immunity.

On an epidemic time scale, it is less clear that vaccine refusal will matter. As long as people who want to be vaccinated are waiting for their turn, the existence of people who don't want to be vaccinated should not matter. On the other hand, both supply and distribution problems should matter. We deal with these issues in Section 3 by introducing several models that incorporate supply and distribution limitations. These models are tested using a variant of the standard SEIR epidemic model with vaccination.

The vaccination model of Section 3 is extended in Section 4 to a COVID-19 scenario, in which individuals are divided into multiple risk classes, with vaccine allocation based on a protocol that favors those at high risk. We conclude this section with an exploration of the impacts of improvements in vaccine acceptance, vaccine manufacture speed, and mitigation practices.

2. Vaccine Refusal in an Endemic Disease Model

Figure 1 shows a schematic that incorporates vaccination, vaccine refusal, loss of immunity, and demographic processes of birth and death into a relatively simple disease model. The class structure is PUIR, a modification of SIR in which the susceptible class is subdivided into (P)revaccinated and (U)nprotected subclasses. We assume a constant total population $N = 1$, achieved via a uniform death rate of μY for each class Y, with no disease-induced deaths, and compensated by a total birth rate μ. Prevaccinated and unprotected individuals become infected at rates βPI and βUI, respectively, and prevaccinated individuals move into the removed class by vaccination at rate ϕP. Infectious individuals

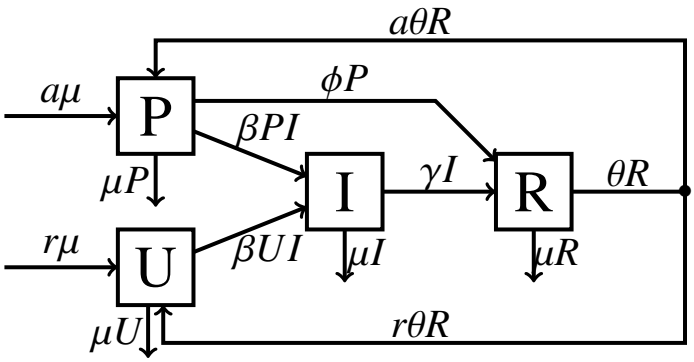

figPUIR

Figure 1. The PUIR endemic model.

are removed at rate γI and removed individuals lose immunity at rate θR. The influx of susceptibles due to both birth and loss of immunity is partitioned into fractions $a + r = 1$, where a is the fraction of individuals who accept vaccination and r the fraction that refuses vaccination. The special cases of no vaccine refusal and no loss of immunity are achieved by setting $r = 0$ and $\theta = 0$, respectively.

While the standard way of writing the model would be to use the mutually exclusive classes P, U, I, and R, it is more convenient to think of the model as having mutually exclusive classes S, I, and R, along with an additional state variable P.* Thus, we have

$$\frac{dP}{dt} = a\mu - \beta PI \qquad - \phi P + a\theta R - \mu P, \tag{2.1}$$ Peqn

$$\frac{dS}{dt} = \mu - \beta SI \qquad - \phi P + \theta R - \mu S, \tag{2.2}$$ Seqn

$$\frac{dI}{dt} = \beta SI - \gamma I \qquad - \mu I, \tag{2.3}$$ Ieqn

$$\frac{dR}{dt} = \gamma I + \phi P - \theta R - \mu R. \tag{2.4}$$ Reqn

To simplify the analysis, we scale the system using the mean infectious duration $1/(\gamma + \mu)$ as the time scale,† resulting in the model (with equations reordered to facilitate use of the next generation method for the basic reproductive number)

$$I' = (\mathcal{R}_0 S - 1)I, \tag{2.5}$$ Ieqn2

$$P' = -\mathcal{R}_0 PI + \epsilon[a - (v+1)P + ahR], \tag{2.6}$$ Peqn2

$$S' = -\mathcal{R}_0 SI + \epsilon[1 - vP - S + hR], \tag{2.7}$$ Seqn2

$$R' = (1-\epsilon)I + \epsilon[vP - (h+1)R], \tag{2.8}$$ Reqn2

where the prime symbol refers to the derivative with respect to scaled time and the new dimensionless parameters are

$$\mathcal{R}_0 = \frac{\beta}{\gamma + \mu}, \qquad v = \frac{\phi}{\mu}, \qquad h = \frac{\theta}{\mu}, \qquad \epsilon = \frac{\mu}{\gamma + \mu} \ll 1. \tag{2.9}$$

*The total susceptible population S figures prominently in the equilibrium and stability analysis.
†The state variables are already scaled by the total population.

Note that $\mathcal{R}_0$ is the basic reproductive number in the absence of vaccination; we will use $\mathcal{R}_v$ for the basic reproductive number with vaccination. The parameters h and v represent the expected number of times an individual loses immunity and receives a vaccination during their lifespan, respectively, and ϵ is the ratio of the mean time in class I to the mean lifespan. The latter is noted as a possible small parameter for asymptotics. Since human infections last weeks while a normal lifespan is measured in years, the numerical value of ϵ is small enough that terms of $O(\epsilon)$ can be neglected when added to terms of $O(1)$.

2.1. Effect of Vaccine Refusal on the Vaccine-Reduced Basic Reproductive Number

Using the next generation method [2, 21], the basic reproductive number in the presence of vaccination is

$$\mathcal{R}_v = S_0 \mathcal{R}_0,$$

where S_0 is the susceptible fraction of the disease-free equilibrium population; thus, S_0 represents the infectiousness of the disease with vaccination, relative to the control case, and serves as one measure of the impact of vaccination and vaccine refusal.

Solution of the algebraic system $P' = R' = 0$ for the disease-free equilibrium $I = 0$ yields the equilibrium removed fraction

$$R_0 = \frac{av}{(1+v)(1+h) - avh}.$$

Conservation of population with $I = 0$ then yields $S_0 = 1 - R_0$, which we can rewrite using $a = 1 - r$ as

$$S_0 = \frac{(1+rv)(1+h)}{(1+rv)(1+h) + av}. \tag{2.10}$$

For further analysis, we assume the public health policy

$$v = 2(1+h)w, \tag{2.11}$$

eqnvh

which means that people will be vaccinated twice plus two times extra for each expected loss of immunity. A full accounting for the impact of vaccination would require a more complicated model that separates out young children from the older population; however, the question at hand is on the impact of vaccine refusal, which will depend less on vaccine administration protocols. Thus, it is reasonable to assume a slightly higher overall level of vaccination than would probably be achieved in practice, but administered without preference for small children. The issue of age-dependent vaccine administration should matter less for diseases with short-lived immunity, such as influenza and (as it becomes endemic) COVID-19; with high values of h the proportion of the prevaccinated class that consists of young children will be small. With (2.11), we obtain

$$S_0 = \frac{1 + 2r + 2rh}{3 + 2rh}. \tag{2.12}$$

The results are illustrated in Figure 2. The panel on the left shows S_0 as a function of the vaccine refusal fraction for different values of the loss of immunity parameter h. At the prescribed vaccination level, the basic reproductive number is reduced to 1/3 of its base value when there is no vaccine refusal. The factor increases to 0.6 with vaccine refusal of 40% for a disease with no loss of immunity. As the

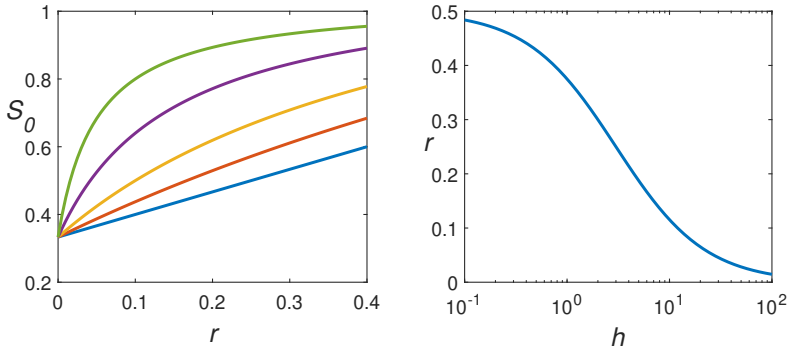

Figure 2. (a) The disease-free susceptible population fraction S_0 for the PSIR model, $h = 0, 1, 3, 10, 30$ (bottom to top); (b) The extent of vaccine refusal corresponding to a vaccine effectiveness reduction by 50%.

figS0_vs_r

rate of immunity loss increases, so does the impact of vaccine refusal. The right panel illustrates this result in a different way by showing the vaccine refusal fraction corresponding to a 50% decrease in vaccine impact ($S_0 = 2/3$). For diseases with lifetime immunity, 50% vaccine refusal reduces vaccine impact by 50%. The impact of refusal increases as the immune duration decreases, to the point where almost any level of vaccine refusal eliminates the public health vaccine benefit for diseases with very short immune duration.

While this model is not intended for COVID-19, it is reasonable to expect that its main results will hold for a more sophisticated model that does fit COVID-19. In light of ongoing vaccine refusal, we can expect that COVID-19 vaccination will have very little public health benefit aside from the individual benefits to those who remain fully vaccinated.

2.2. *Effect of Vaccine Refusal on Infection Prevalence*

If the basic reproductive number is large enough for the endemic disease equilibrium to be stable, then vaccination and vaccine refusal have an effect on the average infectious population. The equilibrium equations show that $I = O(\epsilon)$; thus, the endemic disease equilibrium has

$$S^* = \mathcal{R}_0^{-1}, \qquad R^* = 1 - \mathcal{R}_0^{-1} + O(\epsilon), \tag{2.13}$$

with P^* and $I^* = \epsilon Y^*$ to be determined; note that we are replacing the small quantity I^* with the $O(1)$ quantity Y^*. We define $\rho = I^*/I_0^* = Y^*/Y_0^*$ as the ratio of the vaccine-suppressed infectious population to the infectious population when there is no vaccine. The S' and R' equations then yield the result

$$vP^* = Y_0^* - Y^*, \qquad Y_0^* = (1 + h)R^* \tag{2.14}$$

to leading order. Substituting this result into the P' equation yields a quadratic equation for Y^*:

$$\mathcal{R}_0(Y^*)^2 + (1 + v - \mathcal{R}_0 Y_0^*)Y^* + av(1 + hR) - (1 + v)Y_0^* = 0. \tag{2.15}$$

Our goal here is to calculate the ratio ρ for various values of $\mathcal{R}_0$, h, and $a = 1 - r$, using the public health assumption $v = 2(1 + h)$ from earlier. The results are shown in Figure 3. The bottom curve is the default for the case of no vaccine refusal. The loss of immunity parameter h has no effect because

faster loss of immunity is being compensated by more frequent vaccine administration. When $\mathcal{R}_0 \leq 3$, the vaccine is sufficient to eliminate the endemic equilibrium, but at very high $\mathcal{R}_0$ it is only sufficient to reduce the equilibrium infectious population by about one quarter. Increasing the vaccine refusal rate markedly decreases the benefit of the vaccine, particularly for diseases with relatively low $\mathcal{R}_0$. With vaccine refusal, vaccination is slightly less effective for diseases with faster waning of immunity, but this effect is still largely compensated for by the higher vaccination rate.

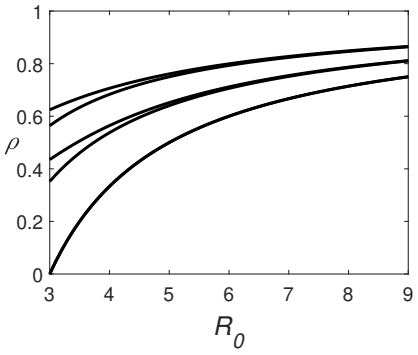

Figure 3. The ratio $\rho = I^*/I_0^*$ of the equilibrium infected population relative to that in the absence of vaccination, with $(r, h) = (0, \text{any}), (0.2, 0), (0.2, 10), (0.4, 0), (0.4, 10)$ from bottom to top.

figratio

3. Vaccination Models with Limited Distribution and Supply

As noted in the introduction, the standard single-phase spontaneous transition model for vaccination fails to account for limited supply and distribution. Here we develop some models that address this flaw.

One complicating factor in modeling vaccination over short time scales is the administration as a two-dose regimen rather than as a single dose. In the context of an epidemiology model, the two-dose regimen adds additional classes, which is a complication unlikely to be important enough to affect overall results. Based on the crude assumption that one dose gives half the protection of the two-dose regimen, we simply count each dose administered as one-half of a vaccination.

3.1. Model Development

As before, let a be the fraction of people who will accept vaccination. With $V(t)$ as the fraction of the population that has been vaccinated (half the number of doses administered since the beginning of vaccination relative to the total population) and $W(t)$ as the fraction of the population that is still waiting for vaccination, we have

$$W(t) = a - V(t). \tag{3.1}$$

eqwv

Our vaccination model will focus on the epidemiological class W, but we can use the model with (3.1) to compute V for parameter fitting against data.

For a first approximation, we could assume that the coefficient in the spontaneous transition rate is

a saturating function of time as the vaccine supply increases; thus,

$$\frac{dW}{dt} = -\Phi^{(1)}(t)W = -\phi g(t)W, \tag{3.2}$$ eqH1

where $\Phi^{(1)}$ is the relative vaccination rate and $0 < g(t) \leq 1$ is a nondecreasing function that accounts for limited supply of vaccine doses during the initial phase of the rollout. As a first approximation, we can assume supply increases linearly up to its maximum; that is,

$$g(t) = \min\left(\frac{t}{\tau}, 1\right), \tag{3.3}$$

where τ is the number of days required to achieve the maximum.

There is good reason to think that this first model will be inadequate. While it accounts for limited supply, it fails to account for limited distribution capacity. For the special case where supply is not limited, we should expect the initial vaccination rate to be largely independent of the number of people waiting to be vaccinated, as it would be limited instead by the number of available vaccination appointments per day. In terms of the process, it is reasonable to think of vaccination as analogous to enzyme kinetics and predation. There is a large pool of patients (substrate/prey) and a finite number of vaccinators (enzyme molecules/predators). Initially, each vaccinator spends nearly all of its time processing patients. Only when the size of the patient pool becomes relatively small do the vaccinators have to spend time searching for patients. This description leads to the supply-adjusted Michaelis-Menten/Holling type 2 model,

$$\frac{dW}{dt} = -\frac{\phi g(t)W}{K + W}, \tag{3.4}$$ eqWH2

with ϕ the theoretical maximum rate of vaccination ('achieved' as $W \to \infty$ and $g = 1$, except that in actuality $W \leq 1$), and K the value of W for which the rate is half of the theoretical maximum. In the context of an epidemic model, it will be convenient to partition this formula into factors as

$$\frac{dW}{dt} = \Phi^{(2)}(W,t)W, \quad \Phi^{(2)}(W,t) = \phi g(t)H_2(W), \quad H_2(W) = \frac{1}{K + W}. \tag{3.5}$$ eqH2

We should also consider the Holling type 3 model,

$$\frac{dW}{dt} = -\frac{\phi g(t)W^2}{K^2 + W^2}, \tag{3.6}$$ eqWH3

or

$$\frac{dW}{dt} = -\Phi^{(3)}(W,t)W, \quad \Phi^{(3)}(W,t) = \phi g(t)H_3(W), \quad H_3(W) = \frac{W}{K^2 + W^2}, \tag{3.7}$$ eqH3

which accounts for the observation in some predator-prey systems that searching can be less efficient when the target population is very low.

Figure 4 shows the fits of the three models to data for the United States [6, 20], with the standard spontaneous transition without vaccine refusal as a control. The best-fit parameters are (using two significant figures unless the first digit is 1)

$$\phi = 0.0050, \quad \tau = 97, \tag{3.8}$$ eqp0

$$\phi = 0.0093, \quad r = 0.29, \quad \tau = 120.5, \tag{3.9}$$ eqp1

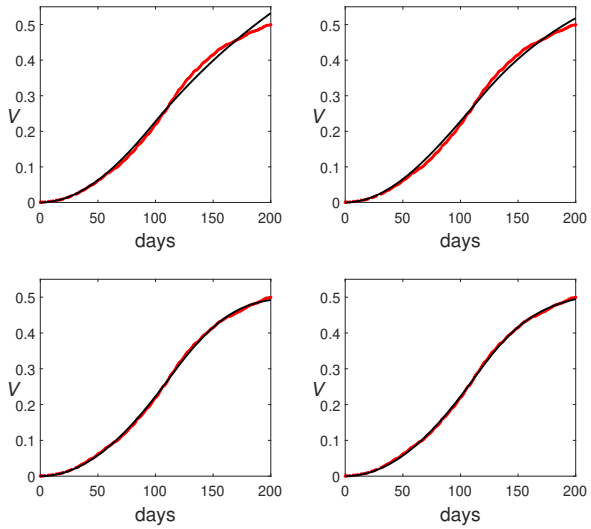

Figure 4. Four supply-limited vaccination models (black) with data for vaccination in the United States from December 20, 2020 through July 7, 2021 (red): top left, (3.2) without vaccine refusal; top right, (3.2); bottom left, (3.4); bottom right, (3.6).

figVax1

$$\phi = 0.0067, \quad r = 0.50, \quad K = 0.115, \quad \tau = 115, \tag{3.10}$$ eqp2

$$\phi = 0.0057, \quad r = 0.45, \quad K = 0.137, \quad \tau = 115 \tag{3.11}$$ eqp3

for the linear (3.2) without vaccine refusal, linear with vaccine refusal, type 2 (3.4), and type 3 (3.6) models, respectively. The linear model without vaccine refusal is a poor match for the data. The linear model with refusal is better, but it clearly shows a systematic error relative to the data and the refusal fraction $r = 0.29$ is objectively too low in comparison to the data. The Holling models show an excellent fit by visual standards. They are almost identical except for a slight difference near the end of the period, when the type 2 model levels off faster than the type 3. The AIC values for the four models are -1634, -1707, -2069, and -2146, respectively, a difference large enough to identify the type 3 model as the best on empirical grounds. Of course the parameters would need to be determined separately for each country, and it is possible that the type 2 model might be better for some. However, the type 3 assumption of slow search rate when the target population is low seems appropriate, so we are justified in preferring type 3 on mechanistic grounds as well as empirical.

3.2. Vaccination in an SEIR Model

To incorporate vaccination into the standard SEIR epidemic model,[‡] we split the susceptible class into prevaccinated and unprotected subclasses, as in Section 2 (Figure 5). For the simplest epidemic model, we neglect processes that occur on a demographic time scale—birth, death, and loss of immunity. For simulations, the initial susceptible population is divided into the P and U subpopulations, each of which subsequently decreases through infection, while the P subpopulation also decreases through vaccination.

[‡]While the SIR model is a good base model for endemic settings, the fact that the time scale for incubation is roughly comparable to that for infectious duration means that the SEIR model is a better base model for epidemic settings.

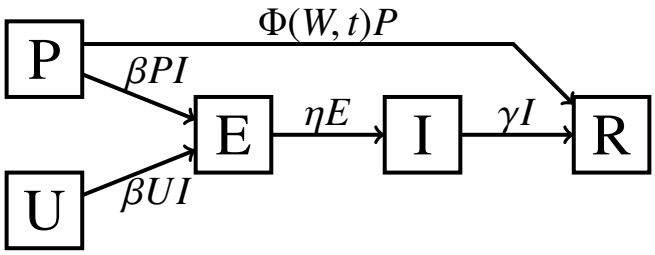

figPUEIR

Figure 5. The PUEIR epidemic model.

We assume (as was the case with COVID-19 in the United States and most other countries) that vaccination is administered without regard for possible prior immunity; hence, a fraction P/W of vaccinations are administered to individuals in the prevaccinated class, which is why the function Φ is the same for the epidemiological model as for the corresponding vaccination model. The full model simply couples the differential equation for W with the epidemic model of the figure,

$$P' = -\beta PI - \Phi(W,t)P, \tag{3.12}$$ P2eqn

$$U' = -\beta UI, \tag{3.13}$$ U2eqn

$$E' = \beta(P+U)I - \eta E, \tag{3.14}$$ E2eqn

$$I' = \eta E - \gamma I, \tag{3.15}$$ I2eqn

$$R' = \gamma I + \Phi(W,t)P, \tag{3.16}$$ R2eqn

using any desired vaccination rate function Φ.

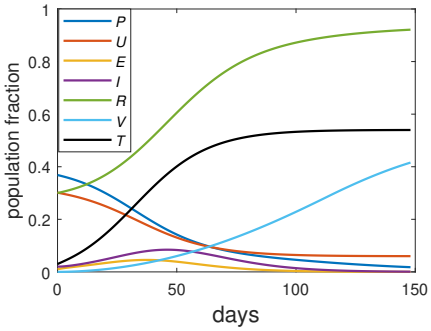

PUEIR_onesim

Figure 6. The PUEIR model with Holling type 3 vaccination (3.7, 3.12–3.16). Parameters are $\gamma = 0.1$, $\eta = 0.2$, $\mathcal{R}_0 = 3$, and vaccination parameters from (3.11), with initial conditions $R(0) = 0.3$, $I(0) = 0.02$, $E(0) = 0.01$, $P(0) = 0.67a$, $U(0) = 0.67r$. T is the cumulative fraction infected, given by $T' = \beta(P+U)I$, $T(0) = E(0) + I(0)$.

Figure 6 shows the result using the Holling type 3 vaccination model (3.7) with best-fit parameters in a scenario with initial conditions of 30% immunity, 2% infectious, and 1% exposed, with an effective basic reproductive number (incorporating any mitigation policies along with the unmitigated basic reproductive number) of 3. The key outcome is that vaccination comes too slowly to make much of a difference. The peak of the infectious class occurs at around day 40, with barely 5% of the population

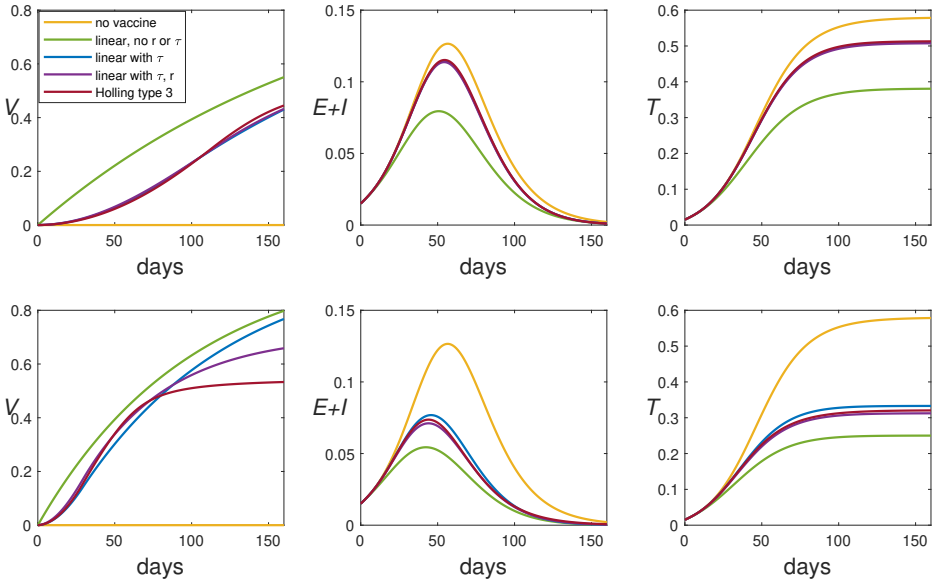

Figure 7. Comparison of vaccination models for two scenarios, both with $\gamma = 0.1$, $\eta = 0.2$, $\mathcal{R}_0 = 3$, $R(0) = 0.3$, $I(0) = 0.1$, $E(0) = 0.05$, and best fit values for r and K; the top panels assume best fit values for ϕ and τ, while the latter assume twice the best-fit values for ϕ and 30 days for τ. The left panels show the fraction of the population that has been vaccinated, the middle panels show the current fraction that is infected, and the right panels show the cumulative fraction infected.

igPUEIR_comp

already vaccinated. The unprotected class levels off around day 75, which is the effective end of the outbreak; meanwhile, the prevaccinated class gradually declines toward 0.

To see what difference the choice of vaccination model makes, we consider two scenarios, shown in Figure 7. We take the same disease parameters of $\gamma = 0.1$, $\eta = 0.2$, and $\mathcal{R}_0 = 3$, along with the best fit values for r and K for each model. The upper panels assume best fit values for the maximum vaccination rate constant ϕ and the time to maximum τ, while the lower panels assume that changes in vaccine research and public health funding allow for a doubling of the maximum rate constant and a reduction of the time to maximum from the 2021 values to 30 days. Initial conditions are $R(0) = 0.3$,[§] $I(0) = 0.1$, $E(0) = 0.05$, with the remaining population split into P and U according to the best fit refusal parameter r.

The top panels show only slight differences between the three models that account for limited supply; that is, vaccine refusal (the two lower curves in the legend) and limited distribution capacity (the bottom curve in the legend) make only a slight difference in the epidemiological outcomes. In the more optimistic scenario of the lower panels, the noticeable difference in the vaccination outcome has some effect on the epidemiological outcomes. In both scenarios, the incorporation of any vaccination into the models clearly affects the model outcomes, while naive vaccination models that fail to account for supply limitations, as represented by the model labeled 'linear, no r or τ,' give epidemiological results that are far too optimistic. Independent of the choice among the three supply-limited vaccination models, the greater supply in the lower scenario clearly makes a large difference in the epidemiological outcomes.

4. A COVID-19 Vaccine Rollout Scenario

Suppose we want to model the introduction of vaccine for COVID-19. The PUEIR model of the previous section is too simple to capture important details of COVID-19. Specifically, we have to be able to account for three different levels of disease—asymptomatic, mild symptomatic, and prehospitalized symptomatic—and we have to be able to account for public health measures such as social distancing, testing, and isolation.

Incorporating vaccination into an earlier SEAIHRD COVID-19 model [15] is more complicated than merely splitting the S class into P and U subclasses. Because COVID-19 involves different levels of risk depending on age and health status, the administration of the vaccine prioritized individuals according to predefined classes. This feature of vaccination needs to be incorporated into a COVID-19 epidemiological model.

4.1. A Model for COVID-19 with Two Risk Classes

The compartment diagram of Figure 8 represents a model for the scenario that occurred when vaccination first became available for COVID-19. The classes are Prevaccinated, Unprotected, Exposed (latent), Asymptomatic, (symptomatic) Infectious, Hospitalized, Removed, and Deceased. Subscripts 1 and 2 are used for low and high risk subclasses for P, U, and E and for standard symptomatic vs prehospitalized subclasses for I. The model incorporates the following assumptions:

1. Susceptible individuals, either prevaccinated or unprotected, become infected at a relative rate

[§]This figure represents the fraction of the population that has become immune through infection prior to the start of the scenario.

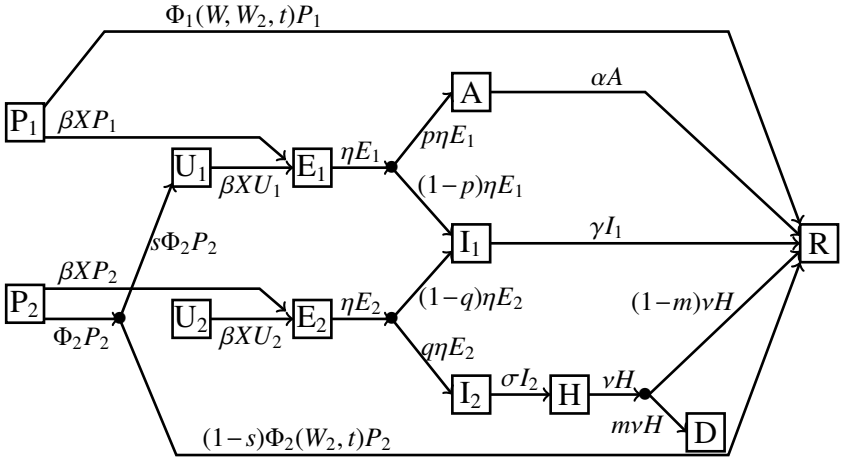

Figure 8. The PUEAIHRD epidemic model.

proportional to an 'effective infectivity' count X. Where the infectious class I is the only class capable of transmitting the disease in an SEIR model, the COVID-19 model has different categories of infectives with different levels of infectivity, which contribute to the effective infectivity in different ways (see below). Public health measures require additional detail.

2. Low-risk latent individuals (E_1) become infectious with relative rate constant η; a fraction p of these become asymptomatic, while the remainder become symptomatic. Similarly, high-risk latent individuals become infectious with relative rate constant η, but here a fraction q become prehospitalized and the remainder symptomatic.[¶]
3. Asymptomatic individuals and mildly symptomatic infectious individuals (A and I_1) gradually recover with relative rate constants α and γ, respectively. Prehospitalized infectives become hospitalized with relative rate constant σ.
4. Hospitalized individuals leave the hospital with relative rate constant ν; a fraction m of these die while the rest recover.
5. Vaccination moves low-risk prevaccinated individuals into the removed class, with relative rate constant that depends on the status of the full vaccination (W) and high-risk vaccination (W_2) programs, as described below. Vaccination moves high-risk individuals into the low-risk unprotected class (U_1) with probability s, or the removed class.[‖]
6. Recovered individuals are immune for long enough that we can ignore possible loss of immunity.
7. Deaths from unrelated causes and births are sufficiently small over the course of the scenario that they can be ignored.

The model consists of the differential equations

$$P_1' = -\beta XP_1 - \Phi_1(W, W_2, t)P_1, \tag{4.1}$$

[¶]The classification of individuals as high or low risk is imprecise at best, so there is no loss of generality in assuming that anyone who becomes asymptomatic must have been low risk, while anyone who becomes hospitalized must have been high risk.

[‖]With these assumptions we can control the extent to which vaccination only reduces severity rather than inducing full immunity. As in the discussion of E_1 and E_2, the lack of precision in categorizing risk levels allows us to assume that all breakthrough cases were among high-risk individuals. The incidence of hospitalization for fully immunized individuals was low enough to justify neglecting that possibility in a relatively simple model.

$$P_2' = -\beta X P_2 - \Phi_2(W_2, t)P_2, \tag{4.2}$$
$$U_1' = s\Phi_2(W_2, t)P_2 - \beta X U_1, \tag{4.3}$$
$$U_2' = -\beta X U_2, \tag{4.4}$$
$$E_1' = \beta X S_1 - \eta E_1, \tag{4.5}$$
$$E_2' = \beta X S_2 - \eta E_2, \tag{4.6}$$
$$A' = p\eta E_1 - \alpha A, \tag{4.7}$$
$$I_1' = (1-p)\eta E_1 + (1-q)\eta E_2 - \gamma I_1, \tag{4.8}$$
$$I_2' = q\eta E_2 - \sigma I_2, \tag{4.9}$$
$$H' = \sigma I_2 - \nu H, \tag{4.10}$$
$$R' = \Phi_1(W, W_2, t)P_1 + (1-s)\Phi_2(W_2, t)P_2 + \alpha A + \gamma I_1 + (1-m)\nu H, \tag{4.11}$$
$$D' = m\nu H, \tag{4.12}$$

COVID-12

where $S = P + U$.

To complete the model, we need to define the quantity X that represents the number of individuals of class I needed to match the total infectivity of the actual population distribution and the functions Φ_j that define the relative rates of the vaccination processes.

4.1.1. Effective infectivity X

Specification of X is based on a number of additional assumptions:

1. Fractions c_i of class I and c_a of class A are identified by a positive test. These confirmed cases have decreased infectivity because they put themselves into isolation.
2. The infectivity of each unconfirmed symptomatic infective is 1 (without loss of generality because there is the additional rate constant β in the transmission rate formula).
3. Asymptomatics and confirmed infectives have infectivities of f_a and f_c (both less than 1) relative to that of unconfirmed symptomatic infectives. Hospitalized infectives do not transmit the disease to an extent that justifies inclusion in the model.
4. There is a 'contact factor' δ that represents the level of risk from the average person's sum total of encounters, relative to normal. This parameter can be used to represent both physical distancing, which decreases the rate of encounters, and wearing of masks, which decreases the risk of each encounter. It is applied to unconfirmed infectives, both symptomatic and asymptomatic, but not to confirmed infectives.

With these assumptions, the effective number of infectives is

$$X = f_c(c_i I + c_a A) + \delta[f_a(1-c_a)A + (1-c_i)I]. \tag{4.13}$$

eqX

4.1.2. A two-risk-class supply-and-distribution-limited vaccination model

With the population divided into low risk and high risk classes (subscripts 1 and 2, respectively), our best fit model for the population of vaccine accepters from before (W from (3.5) or (3.7)) should still apply to the sum $W = W_1 + W_2$; we need only prescribe a model for W_2 and then calculate Φ_1 from

$W_1' = W' - W_2'$. The simplest assumption is that the same model holds for W_2 as for W, with the same parameter K:

$$W_2' = -\Phi_2(W_2, t)W_2, \quad \Phi_2(W_2, t) = \phi g(t) H_j(W_2), \tag{4.14}$$ eqW2

where j is 2 or 3.

While we do not need to keep track of W_1 as a differential equation state variable, we do need to determine Φ_1 from

$$\Phi_1(W, W_2, t) = -\frac{W_1'}{W_1} = -\frac{W' - W_2'}{W_1} = \phi g(t) \frac{H_j(W)W - H_j(W_2)W_2}{W_1}. \tag{4.15}$$

Using the formulas for H_j, we obtain

$$\Phi_1^{(2)}(W, W_2, t) = \frac{\phi K g(t)}{(K + W)(K + W_2)} \tag{4.16}$$

for type 2 and

$$\Phi_1^{(3)}(W, W_2, t) = \frac{\phi K^2 g(t)(W + W_2)}{(K^2 + W^2)(K^2 + W_2^2)}. \tag{4.17}$$ eqPhi1

for type 3. To complete the vaccination models, we assume a fraction h of the population falls into the high-risk category and that the vaccine refusal fractions are r for the general population and $r_2 < r$ for the high-risk subpopulation. Initial conditions are then

$$W(0) = 1 - r, \qquad W_2(0) = h(1 - r_2). \tag{4.18}$$ vaxic

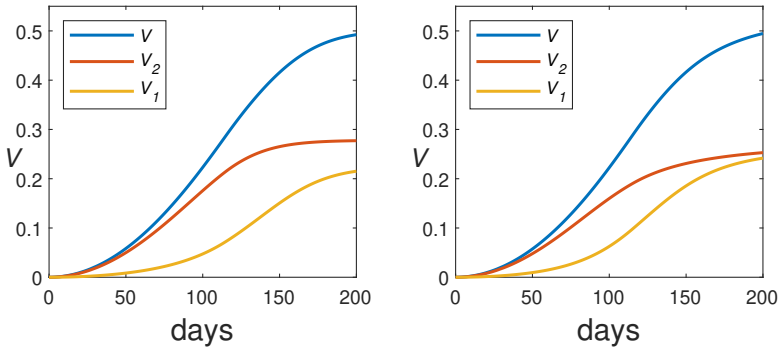

Figure 9. The two-class vaccination model using (3.4) for W and W_2 (left) and (3.6) (right) and initial conditions (4.18), with $h = 0.333$, parameters ϕ, r, K, and τ from the best fits for V (3.10–3.11), and $r_2 = r/3$. The plots show the vaccinated fractions $V_j = W_j(0) - W_j$. figVax2

Figure 9 compares the two-class vaccination models with Holling type 2 and 3 dynamics. There is no suitable data that separates vaccination for high-risk and low-risk classes, particularly since risk levels do not exactly correspond to CDC priority classes. However, there are qualitative differences that can help us choose between the two models; in particular, the type 2 model shows a higher efficiency in directing vaccination to high-risk individuals than the type 3. Some inefficiency clearly occurred anecdotally, as the author's limited acquaintances include several low-risk individuals who were vaccinated early because some health-care facilities chose to vaccinate people of any risk class rather than waste defrosted doses. The type 2 model shows high-risk vaccination to have been completed within 4 months, a claim that is likely overoptimistic; thus, the type 3 model seems slightly better.

parameter	meaning	value	ref's	notes
$\mathcal{R}_0$	basic reproductive number	7		5
h'_0	initial hospitalization rate per 100K	1	[7]	2
r_0	initial R	0.3		2
c_a	confirmed fraction for A	0.2		2
c_i	confirmed fraction for I	0.7		2
f_a	relative infectivity of A	0.75	[5]	
f_c	relative infectivity in isolation	0.1		2
h	high-risk fraction	0.333		2
K	vaccination semi-saturation const.	0.137		1
m	deaths per H	0.2	[9]	
p	low-risk asymptomatic fraction	0.6	[5]	4
q	high-risk prehospitalization fraction	0.06	[5, 9]	4
r	overall vaccine refusal probability	0.45, 0.15		1
r_2	high-risk vaccine refusal probability	0.15, 0.05		3
s	breakthrough probability for high risk	0.3		4
α	clearance rate for A (1/days)	0.125	[3]	
γ	clearance rate for I_1 (1/days)	0.1	[11, 17]	
δ	contact factor	0.5		2
η	clearance rate for E (1/days)	0.2	[13]	
ν	clearance rate for H (1/days)	0.1	[16]	
σ	clearance rate for I_2 (1/days)	0.333	[10]	
τ	time to maximum vax. supply	115, 60		1
ϕ	vaccination rate constant	0.0057		1

table1

Table 1. Parameter Values for PUEAIHRD simulation

4.2. Numerical Experiments

To test the impact of vaccination in a critical scenario, we consider a hypothetical scenario in which vaccination begins in the United States in September 25, 2020, at a period of low chronic incidence just prior to a significant spike in cases, rather than starting 3 months later in the middle of a spike, as actually happened. Parameters are listed in Table 1. The notes column refers to the following list of comments:

1. Primary value fit from US data, as shown above. Secondary values are either optimistic guesses for countries with less vaccine refusal or optimistic guesses for vaccine supply in future pandemics.
2. These are guesses for parameters that cannot be measured or are strongly dependent on region or jurisdiction. The full set of these parameters has been tuned so that the results for the no vaccination case (the red curve in Figure 10) roughly match the actual results for new hospitalizations [7], which should be the quantity σI_2. This quantity is initially given per 100,000 people as the parameter $h'_0 = 1$ and shows a peak in the dataset of about 5 times that value after about 110 days.
3. Values for r_2 are 1/3 of the values for r in any simulation. This assumption is suggested by US

age-stratified vaccination data [6].

4. These parameter values are calculated by combining h with overall population estimates of 40% asymptomatic, 3% hospitalized, and 10% infection probability for vaccinated patients.
5. A large range of values of $\mathcal{R}_0$ has been reported for the ancestral strain, with values in the range $[2.5, 3]$ most common. These are clearly too low, as they cannot account for the growth of hospitalizations in March 2020 [7] nor the observation that masking and social distancing greatly reduced the incidence of seasonal flu and rhinoviruses (having $\mathcal{R}_0 \geq 2.5$), without keeping COVID under control.** The best estimate for the ancestral strain is $\mathcal{R}_0 = 5.8$ for the United States and slightly less for Europe [12]. Because of the large spike in cases for the time period of our scenario, it seems probable that the basic reproductive number at this time had increased, either because a more infectious strain was already taking over or because of seasonal changes in contact patterns.

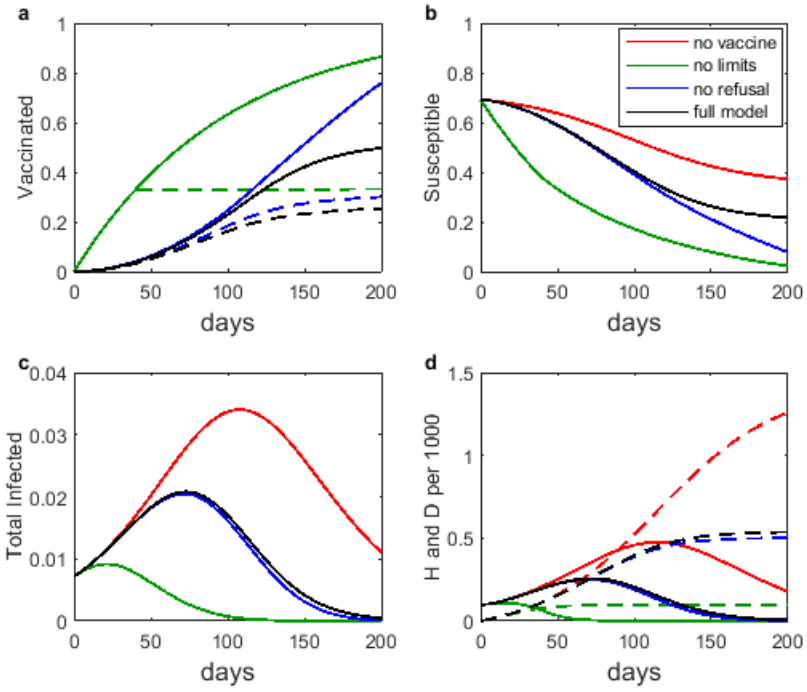

Figure 10. The PUEAIHRD model with various vaccination submodels: no vaccine, spontaneous transition, Holling type 3 with no vaccine refusal, and the full Holling type 3 model; (a): vaccinated fraction (solid) and high-risk vaccinated fraction; (b) total susceptible fraction; (c) total infected fraction; (d) hospitalized (solid) and deceased per thousand.

UEAIHRD_test

4.2.1. Impact of vaccination model selection

Figure 10 shows the results of an experiment to test the effects on model behavior of four different vaccination model choices:

**Global market reports for over-the-counter cold remedies show a significant decline in the winter of 2020-2021 in spite of the use of these medications by COVID patients [8]. The only explanation is that incidence of seasonal rhinovirus was much less than in the prior year.

1. No vaccination;
2. The naive spontaneous transition model with the additional naive assumption that all high-risk individuals are vaccinated before any low-risk individuals, using $\phi = 0.01$, corresponding to a 100-day mean time for vaccination;
3. The two-class Holling type 3 vaccination model (3.6, 4.14) with best-fit parameters for ϕ, K, and τ, but neglecting vaccine refusal;
4. The two-class Holling type 3 vaccination model with best-fit values for all parameters.

The no-vaccine scenario shows a significant wave of cases, as happened in the actual event, with correspondingly high hospitalizations and deaths. The naive vaccination model shows vaccination having a dramatic impact on this wave; however, the vaccination plot in panel **a** shows how unrealistic this is. With a better vaccination model, we see that vaccination would have had a significant positive impact, but much less than the impact seen with the naive model.

The impact of vaccine refusal is larger here than in the PUEIR model example because the prioritization of high-risk individuals makes vaccine refusal significant earlier in the scenario. The difference between the no refusal and full model results for vaccine doses administered to high-risk individuals becomes noticeable on the panel **a** graph at about 70 days. This is not enough to significantly affect the total number infected in panel **c**, but it does make a visual difference in the hospitalization and death counts of panel **d**. Future spikes for scenarios starting after the displayed one will play out quite differently because the total susceptible population drops to a far greater extent with no vaccine refusal (panel **b**).

4.2.2. Impact of vaccination model parameters

We now use the PUEAIHRD epidemic model with the two-class supply-limited Holling type 3 vaccination model to explore the impact of several key parameters that can be influenced by public policy decisions. Figure 11 shows the results. There are six combinations of assumptions:

1. The default scenario, in which there is no vaccination;
2. The base scenario, in which vaccination parameters are from the best-fit values and the contact factor is $\delta = 0.5$;
3. The enhanced acceptance scenario, in which vaccine refusal is reduced by a factor of 3, equivalent to replacing the United States with one of the countries having highest vaccine acceptance in 2021;
4. The enhanced manufacture scenario, in which advance preparation reduces the time required for vaccination to reach full capacity from 115 days to 60 days;
5. The combined enhancement scenario, combining reduced vaccine refusal with faster achievement of capacity;
6. The enhanced mitigation scenario, in which vaccine parameters are not enhanced, but the contact factor is reduced from 0.5 to 0.4.

Panel **a** shows the vaccination outcomes for the different scenarios. Enhanced acceptance raises the overall vaccination numbers at the end of the scenario, while enhanced manufacturing leads to an earlier approach to those maxima. The curve for scenario 6 is omitted, as it is the same as that for scenario 2.

Panel **b** shows the time history of the total susceptible population. Of primary interest are the values at the end of the scenario, as these values are predictors of the severity of the next outbreak of the same

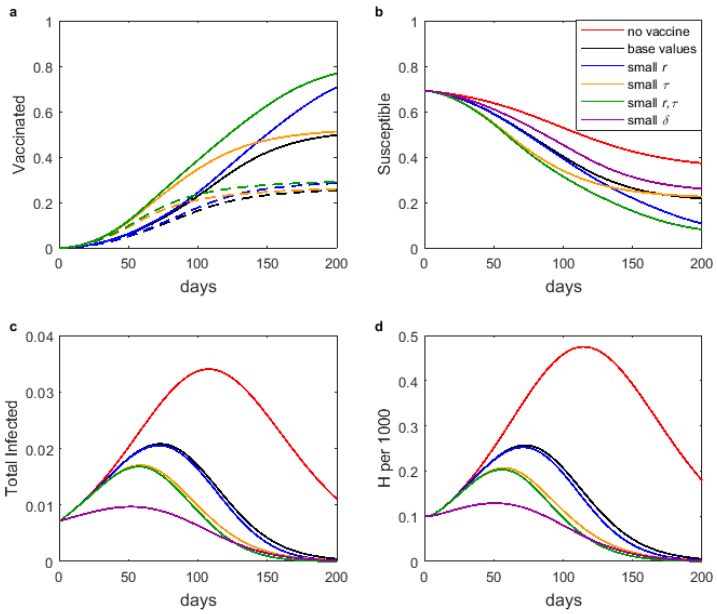

Figure 11. The PUEAIHRD model with various assumptions about vaccination and mitigation: no vaccine, base parameter set, less refusal, faster rollout, less refusal and faster rollout, base parameter set with lower contact factor; (a): vaccinated fraction (solid) and high-risk vaccinated fraction; (b) total susceptible fraction; (c) total infected fraction; (d) hospitalized per thousand.

EAIHRD_test2

disease. Here we see the value of enhanced vaccine acceptance.

Panels **c** and **d** show the time histories of the total infected and hospitalized. Enhanced vaccine acceptance makes only a small difference in these outcomes, while enhanced ramping speed makes a much larger difference. The effect of a modest improvement in the standard mitigation practices of social distancing and masking is larger than the impact of enhancements to vaccination, however.

The graphs of total cases and total hospitalized are almost identical aside from the scale, except for one noticeable difference. In general, vaccination has a greater effect on hospitalization than it has on infection in our COVID-19-based scenario; this is clearly due to a combination of prioritization of high-risk individuals for vaccination combined with the large probability that vaccination of these individuals reduces the severity of the disease without reducing the incidence.

5. Discussion and Conclusions

COVID-19 has provided an ideal opportunity to develop modeling tools that can be adapted to new diseases. One area where previous models fall short is the incorporation of vaccination subject to vaccine refusal and limitations on supply and distribution. The models developed in this paper will likely be suitable for novel disease pandemics of the future. They are more complicated than the standard single-phase transition model, so it is important to be clear about the benefits.

5.1. Vaccine Refusal

As of April 2022, the fractions of national populations that have received a full initial vaccine protocol (not counting boosters) is as high as 96% in the United Arab Emirates, but with a worldwide average of only 59% [19]. The actual percentages of people who have been fully protected at any given time are surely smaller, as the initial protocol without boosters was no longer adequate in April 2022. In some cases, the main difficulty is global inequity, but in other cases, such as the United States (just 66% of people having had the full initial protocol), the problem is significant levels of resistance to vaccination. This resistance will likely be present for novel diseases of the future, so it is important to account for it in models. This requires models that partition the standard susceptible class into prevaccinated and unprotected classes. Of course the extra state variable adds additional complexity to a model, which should be avoided when the extra detail is not necessary.

For an endemic disease, the benefits of vaccination are significantly reduced by widespread vaccine refusal, as illustrated in Figures 2 and 3. As one would expect, this effect is particularly important for diseases where immunity is short-lived and vaccination must be renewed regularly. Here, vaccine resistance will be augmented by apathy among people who lose interest in renewing their immunity. The public health benefits of vaccination are minimal for diseases with immunity that lasts only a few years or less or for societies with significant levels of vaccine resistance.

Vaccine refusal is largely irrelevant in many vaccine rollout scenarios, as there are not enough doses at first to fully accommodate those who want to be vaccinated. As more doses become available and more people are vaccinated, vaccine refusal begins to have an impact. As shown in Figures 10 and 11, vaccine refusal by high-risk individuals makes a noticeable difference in hospitalizations and deaths, although neither vaccine refusal in general nor that specifically for high-risk individuals makes much difference to the overall course of the pandemic.

5.2. *Supply and Distribution*

Supply and distribution issues are critical in epidemic scenarios, when there is a large queue of people wanting vaccination and limited numbers of doses and appointment slots. The significant difference between the outcomes of the naive vaccination model and more realistic models, as seen in Figure 10, clearly shows the necessity of using a realistic vaccination model.

In terms of good public health outcomes, it is more important in the epidemic stage of a disease to have a good infrastructure for manufacture and administration than it is to increase vaccine acceptance, as seen in the better performance of scenarios with enhanced rollout speed compared to scenarios with enhanced acceptance in Figure 11. By the time a disease has become endemic, however, most people only need vaccination when they are due for a booster, so we can expect doses and appointment slots to be adequate. Endemic disease scenarios do not require the more sophisticated accounting for supply and distribution that is needed for epidemic scenarios.

5.3. *Maintaining Mitigation*

The comparison of scenarios in Figure 11 shows that even with the most optimistic vaccination parameters, the effect of a small decrease in contact factor is greater than the effect of vaccination by itself. While quickly eliminating unpopular mitigation practices makes for good politics, it is much better for public health outcomes to delay elimination of these practices until vaccination has become widespread enough to make a difference. This observation is self-evident, but modeling such as has been done here serves to offer quantitative predictions.

References

arino 1. J. Arino, S. Portet, A simple model for COVID-19, *Infectious Disease Modelling*, **5** (2020), 309–315, DOI: 10.1016/j.idm.2020.04.002.

brauer 2. F. Brauer, C. Castillo-Chavez, Z. Feng, *Mathematical Models in Epidemiology*. Springer-Verlag, New York, 2019.

byrne 3. A.W. Byrne, D. McEvoy, A.B. Collins, K. Hunt, M. Casey, A. Barber, F. Butler, J. Griffin, E.A. Lane, C. McAloon, K. O'Brien, P. Wall, K.A. Walsh, S.J. More, Inferred duration of infectious period of SARS-CoV-2: rapid scoping review and analysis of available evidence for asymptomatic and symptomatic COVID-19 cases, *BMJ Open*, **10** (2020), https://doi.org/10.1136/bmjopen-2020-039856.

cai 4. L.-M. Cai, Z. Li, X. Song, Global analysis of an epidemic model with vaccination, *J. Appl. Math. Comp.*, **57** (2018), 605–628, https://doi.org/10.1007/s12190-017-1124-1.

cdc 5. The Centers for Disease Control and Prevention, *COVID-19 Pandemic Planning Scenarios*, 2020. Available from https://www.cdc.gov/coronavirus/2019-ncov/hcp/planning-scenarios.html#five-scenarios.

cdcvax 6. The Centers for Disease Control and Prevention, *COVID-19 Vaccinations in the United States*, 2022. Available from https://covid.cdc.gov/covid-data-tracker/#vaccinations_vacc-total-admin-rate-total.

cdchosp 7. The Centers for Disease Control and Prevention, *New Admissions of Patients with Confirmed COVID-19, United States*, 2022. Available from `https://covid.cdc.gov/covid-data-tracker/#new-hospital-admissions`.

market 8. *Cough and Cold Preparations Global Market Report 2021: COVID-19 Implications and Growth to 2030*. The Business Research Company, 2021.

ctp 9. The COVID Tracking Project. *Our Data*, 2020. Available from `https://covidtracking.com/data`.

faes 10. C. Faes, S. Abrams, D. Van Beckhoven, G. Meyfroidt, E. Vlieghe, N. Hens, Time between symptom onset, hospitalisation and recovery or death: statistical analysis of Belgian COVID-19 patients. *Int J Environ Res and Public Health*, (2020), doi: 10.3390/ijerph17207560.

he 11. X. He, E.H.Y. Lau, P. Wu, X. Deng, J. Wang, X. Hao, Y.C. Lau, J.Y. Wong, Y. Guan, X. Tan, X. Mo, Y. Chen, B. Liao, W. Chen, F. Hu, Q. Zhang, M. Zhong, Y. Wu, L. Zhao, F. Zhang, B.J. Cowling, F. Li, G.M. Leung, Temporal dynamics in viral shedding and transmissibility of COVID-19, *Nat Med*, **26** (2020), 672–675, doi: 10.1038/s41591-020-0869-5.

ke 12. R. Ke, E. Romero-Severson, S. Sanche, N. Hengartner. Estimating the reproductive number $\mathcal{R}_0$ of SARS-CoV-2 in the United States and eight European countries and implications for vaccination. *J. Theo. Biol.*, **517** (2021), doi: 10.1016/j.jtbi.2021.110621.

lauer 13. S.A. Lauer, K.H. Grantz, Q. Bi, F.K. Jones, Q. Zheng, H.R. Meredith, A.S. Azman, N.G. Reich, J. Lessler, The incubation period of coronavirus disease 2019 (COVID-19) from publicly reported confirmed cases: estimation and application. *Annals of Internal Medicine*, (2020), doi: 10.7326/M20-0504.

mmee 14. G. Ledder, *Mathematical Modeling for Epidemiology and Ecology*, 2nd edition, Springer-Verlag, New York, in press.

primus 15. G. Ledder, M. Homp, Using a COVID-19 model in various classroom settings to assess effects of interventions, *PRIMUS*, **32** (2021), 278–297, DOI: 10.1080/10511970.2020.1861143.

lewnard 16. J.A. Lewnard, V.X. Liu, M.L. Jackson, M.A. Schmidt, B.L. Jewell, J.P. Flores, C. Jentz, G.R. Northrup, A. Mahmud, A.L. Reingold, M. Petersen, N.P. Jewell, S. Young, J. Bellows, Incidence, clinical outcomes, and transmission dynamics of severe coronavirus disease 2019 in California and Washington: prospective cohort study, *BMJ*, **369** (2020), doi: 10.1136/bmj.m1923.

liu 17. Y. Liu, L.-M. Yan, L. Wan, T.-X. Xiang, A. Le, J.-M. Liu, M. Peiris, L.L.M. Poon, W. Zhang, Viral dynamics in mild and severe cases of COVID-19, *Lancet Infect Dis* **20** (2020), 656–657, doi: 10.1016/S1473-3099(20)30232-2.

artcheva 18. M. Martcheva, *An Introduction to Mathematical Epidemiology*. Springer-Verlag, New York, 2015.

ataworld 19. Our World in Data, *Coronavirus Vaccinations*, 2022. Available from `https://ourworldindata.org/covid-vaccinations`.

vaxdata 20. Our World in Data, *State-by-state Data on COVID-19 Vaccinations in the United States*, 2022. Available from `https://ourworldindata.org/us-states-vaccinations`.

nextgen 21. P. van den Driessche, J. Watmough, Reproduction numbers and sub-threshold endemic equilibria for compartmental models of disease transmission, *Math. Biosci.*, **180** (2002), 29–48, doi: 10.1016/S0025-5564(02)00108-6.

AIMS Press